A&A 432, 699–704 (2005)
DOI: 10.1051/0004-6361:20041366

Astronomy & Astrophysics

On the formation of the He I 10 830 Å line in a flaring atmosphere

M. D. Ding[1], H. Li[2], and C. Fang[1]

[1] Department of Astronomy, Nanjing University, Nanjing 210093, PR China
[2] Purple Mountain Observatory, Chinese Academy of Sciences, Nanjing 210008, PR China

Received 28 May 2004 / Accepted 1 November 2004

Abstract. We explore the formation of the He I 10 830 Å line in a flaring atmosphere, with special attention to the nonthermal effects of an electron beam. Using non-LTE calculations we obtain the line profiles from different model atmospheres. Without the nonthermal effects, the line changes from weak absorption in a cool atmosphere to emission in a hot and condensed atmosphere, as expected. However, the presence of an electron beam can significantly change the line strength, producing much stronger absorption and emission in these two cases. We find that in the nonthermal case, the collisional ionization of He I followed by recombinations becomes an important process in populating the triplet levels corresponding to the He I 10 830 Å line. These results suggest that the He I 10 830 Å line is also a potential diagnostic tool for nonthermal effects in solar or stellar flares.

Key words. line: profiles – Sun: atmosphere – Sun: flares – stars: atmospheres

1. Introduction

Although the He I 10 830 Å line is much weaker than some chromospheric lines such as Hα or Ca II H and K, it remains an important line in the spectroscopy of solar active phenomena. The formation of this line in the solar atmosphere has been studied by many authors (e.g., Milkey et al. 1973; Shine et al. 1975; Fontenla et al. 1993; Andretta & Jones 1997, hereafter AJ97; Labrosse & Gouttebroze 2001). The He I 10 830 Å line involves two triplet levels with several distinguishing features. The lower level of this line ($1s2s\ ^3S$) is a metastable level which is about 20 eV above the ground state ($1s^2\ ^1S$). Therefore, electric dipole transition is forbidden between them. In order to produce enough populations at the metastable level, two distinct mechanisms have been proposed, namely, the photoionization-recombination mechanism (PRM) and the collisional mechanism (CM). The former assumes that the EUV radiation coming back from the corona leads to an overionization of He I in the chromosphere ($T \lesssim 10\,000$ K), followed by a recombination to excited levels. Direct collisional excitation from the ground state occurs in a relatively hotter material ($T \gtrsim 20\,000$ K). These two mechanisms are usually difficult to distinguish in the formation of the He I 10 830 Å line (Sasselov & Lester 1994). A detailed discussion on their application to the solar atmosphere can be found in AJ97. On the other hand, the upper level of the line ($1s2p\ ^3P^o_{2,1,0}$) is J-splitting, so that the line is a multiplet with components at 10 830.341, 10 830.250, and 10 829.081 Å, respectively. The first two components blend together while the third is usually distinguishable.

In the solar disk, the He I 10 830 Å line appears as a weak absorption line in the continuum background. Its absorption depth increases with increasing coronal EUV irradiation (e.g., Avrett et al. 1994; AJ97). Only at the site of a very strong flare does the line turn to emission. This needs the atmosphere to be highly heated and condensed, as reflected in the semi-empirical model F2 proposed by Machado et al. (1980).

Considering the specific features of the He I 10 830 Å line and its potential role in the spectroscopy of solar flares (e.g., Li et al. 1996; You et al. 1998), we need to know how the line changes with different physical conditions in a flaring atmosphere. When a flare occurs, the flaring atmosphere is heated to a higher temperature; at the same time, some chromospheric material is driven to flow into the corona (chromospheric evaporation), thus making the chromosphere more condensed. This process can be visually seen from the change in semi-empirical models, e.g., from the quiet-Sun model VAL-C (Vernazza et al. 1981) to flare models F1 and F2 (Machado et al. 1980). On the other hand, it is known that flares are usually heated by energetic electrons. The impact on the atmosphere by a beam of nonthermal electrons not only produces direct heating, but also changes the line and continuum emission through nonthermal ionization and excitation of neutral atoms. Studies have shown that the hydrogen Lyman lines (Hénoux et al. 1995), the Balmer and Ca II lines (Fang et al. 1993), the EUV continuum (Ding & Schleicher 1997), the optical continuum (Ding et al. 2003), and even the SOHO/MDI Ni I 6768 Å line (Ding et al. 2002) can be changed by the nonthermal effects to an extent that is of course different from case to case. However, it is still unknown how the He I 10 830 Å line responds to the bombardment of a

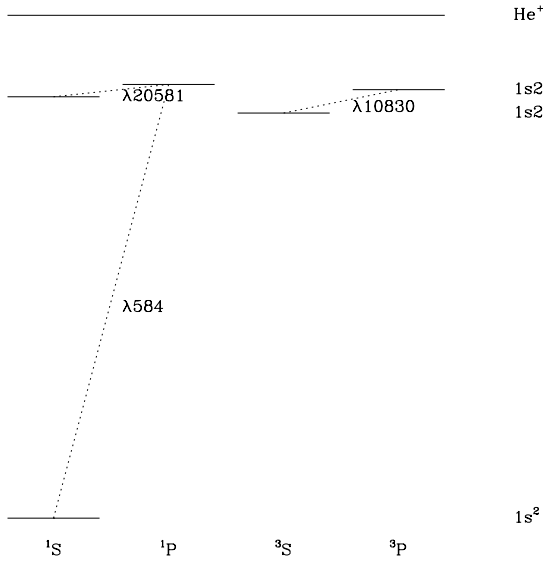

Fig. 1. Schematic diagram showing the atomic model of He I comprising the five lowest bound levels plus continuum.

nonthermal electron beam. In this paper, we study this issue by making non-LTE calculations of model atmospheres. We introduce the basic computational method in Sect. 2, present the results in Sect. 3, and give our conclusion in Sect. 4.

2. Computational method

2.1. The model atom

The model atom for He I adopted here consists of the five lowest levels (with principal quantum number $n \leq 2$) plus the ground state of He II. The level energies are from Martin (1987). There are only three permitted radiative transitions between these levels (Fig. 1), the oscillator strengths of which are given by Kono & Hattori (1984). Line broadening data are from Griem (1974) and Dimitrijević & Sahal-Bréchot (1984). The collisional excitation rates, collisional ionization rates, and photoionization cross-sections are computed according to Benson & Kulander (1972), Mihalas & Stone (1968), and Fernley et al. (1987).

As was done in AJ97, we do not consider the fine structure of the $1s2p\ ^3P^o$ state when solving the rate equations. The occupation number at this state is finally distributed to each sublevel according to its statistical weight in order to compute the emergent He I 10 830 Å line. This simplification is valid when collisional transitions between sublevels are so frequent as to maintain such a distribution. Radiative transitions may violate this distribution only when the multiplet components show quite different intensities. This could happen in the solar atmosphere where the multiplet components are formed at different depths. However, as will be demonstrated below, the He I 10 830 Å line is mostly formed in a relatively dense medium, which guarantees enough collisions between sublevels to make the simplification still viable.

2.2. The model atmospheres and the effect of the nonthermal electron beam

We select three model atmospheres: the quiet-Sun model, VAL-C (Vernazza et al. 1981), and the flare models, F1 and F2 (Machado et al. 1980), to represent different events or different heating status of the flaring atmosphere. Also, we introduce a nonthermal electron beam bombarding the atmosphere in association with the flare impulsive heating.

As was discussed in Fang et al. (1993), the electron beam can cause nonthermal excitation and ionization of the neutral atoms. Therefore, the statistical equilibrium equation becomes

$$\sum_{j\neq i}^{N} n_j \left(R_{ji} + C_{ji} + C^B_{ji}\right) - n_i \sum_{j\neq i}^{N} \left(R_{ij} + C_{ij} + C^B_{ij}\right) = 0, \qquad (1)$$

where R_{ij} and R_{ji} are radiative transition rates that are computed according to the formulae described in Mihalas (1978), C_{ij} and C_{ji} are thermal collisional rates, and C^B_{ij} and C^B_{ji} are nonthermal collisional rates. The total level number N is 6 for the atomic model of He I adopted here (including the bound levels plus the continuum). Therefore, the magnitude of the nonthermal term determines the change of the level populations with respect to the thermal case. For a beam with a power law distribution, Fang et al. (1993) have derived the formulae to calculate the nonthermal collisional rates for hydrogen and ionized calcium. For the He I atom, we can evaluate the nonthermal ionization rate through a comparison between the cross-sections of collisional ionization of H and He I by energetic electrons. Assuming a mean electron energy of ~30 keV, we find $\sigma_{\rm He}/\sigma_{\rm H} \simeq 1.2$[1]. Therefore, the nonthermal ionization rate for He I is derived as

$$C^B_{1c}({\rm He}) \simeq 1.2 C^B_{1c}({\rm H}) \simeq 2.08\times 10^{10}\Phi/n_1({\rm H}), \qquad (2)$$

where n_1(H) is the hydrogen ground level population, and Φ is the energy deposit rate in the atmosphere by the electron beam (see the formula in Ding & Fang 2000). The nonthermal ionization rate is then included in the rate equations for He I, as has been done for hydrogen in previous studies.

The nonthermal excitation rates of He I can be estimated in the same way. However, we lack reliable data for cross-sections of collisional excitation by ~30 keV electrons. A comparison between the cross-section of collisional ionization and that of collisional excitation to the triplet levels of He I by ~3 keV electrons reveals that the latter is four times smaller than the former. If this applies to the case of deka keV electrons, the effect of nonthermal excitation should be much smaller than the effect of nonthermal ionization. This has been confirmed by test computations. Therefore, in the following computations, we only consider the effect of nonthermal ionization.

We then solve the coupled equations of statistical equilibrium and radiative transfer, together with the hydrostatic equilibrium equation, for model atmospheres. The three lines at 584, 10 830, and 20 581 Å and the five continua are all treated with detailed radiative transfer equations. Therefore, the nonlocal effects are taken into account consistently.

[1] According to data provided by National Institute of Standards and Technology (NIST), available at the URL `http://physics.nist.gov/PhysRefData/Ionization/index.html`

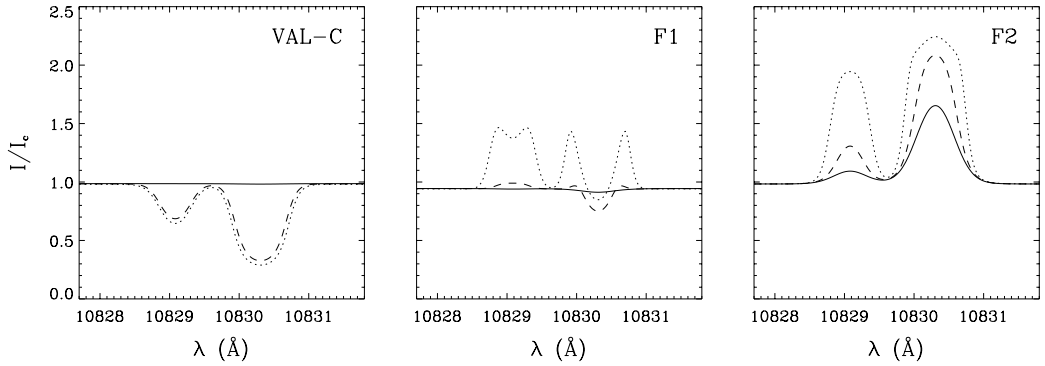

Fig. 2. Line profiles of He I 10 830 Å depending on the atmospheric models and the effect of a nonthermal electron beam. *From left to right*, the three panels refer to three atmospheric models: VAL-C (Vernazza et al. 1981), F1 and F2 (Machado et al. 1980). The solid lines refer to the case without an electron beam, while the dashed and dotted lines refer to the cases with electron beams whose energy fluxes are 10^9 and 10^{10} erg cm^{-2} s^{-1}, respectively. The profiles are computed at solar disk center and normalized to the nearby continuum.

2.3. Limitation of the model

As is well known, the He I 10 830 Å line is very sensitive to the coronal EUV irradiation. In our calculations, we use the semi-empirical models VAL-C for the quiet-Sun, F1 for a weak flare, and F2 for a strong flare. The EUV irradiations computed from these models are quite different and have been consistently incorporated in the calculations of the He I 10 830 Å line. However, the EUV irradiation during flares should change rapidly and exerts a great influence on the line profile. Generally speaking, the effect of an enhanced coronal irradiation is to strengthen the He I 10 830 Å line owing to an enhanced PRM. In some sense, this effect cannot be easily distinguished from the effect of nonthermal electrons. In the present work, we restrict our attention to the role of nonthermal electrons. A combination of both factors will be studied in a future work.

The model atom for He I adopted here is rather simple with only five bound levels. Including more bound levels can yield more quantitatively accurate results. We postulate that recombinations to other bound levels can reduce somewhat the populations at the triplet levels and thus the strength of the He I 10 830 Å line. However, the results on the nonthermal effects drawn below are qualitatively valid, considering that our purpose is not to reproduce exactly the observed line profiles, but only to show the role of nonthermal electrons.

3. Computations and discussions

3.1. Computational results

We make non-LTE calculations for the three model atmospheres mentioned above with and without a nonthermal electron beam. The line profiles are plotted in Fig. 2. We notice that, if there is no nonthermal electron beam, the He I 10 830 Å line appears in very weak absorption in the quiet-Sun model, then the line depth increases in the F1 model and it finally changes to an emission line in the F2 model. The effect of the nonthermal electron beam is, however, quite obvious in changing the line strength. In the quiet-Sun model, the presence of an electron beam can result in a rather strong absorption profile, in contrast to the weak absorption one in the case of no electron beam. In the F1 model, the profile changes from absorption to emission, depending on the energy flux of the electron beam. In the F2 model, the profile is always in emission; however, the electron beam can make the profile much stronger.

The above results can be explained by checking the formation process of the He I 10 830 Å line. For this purpose, we plot in Fig. 3 the line source function and the optical depth at line center (referring to the center of the strongest component) for all the above cases. We first discuss the case of no electron beam. As was indicated by Avrett et al. (1994), the He I 10 830 Å line is optically thin in the chromosphere of the quiet-Sun region which produces only a weak absorption in the line. Changing from the quiet-Sun to the flare models, the chromospheric contribution to the line increases. The reason is that, on one hand, a flaring atmosphere produces an enhanced EUV irradiation responsible for the photoionization of He I and, on the other hand, the heated and condensed material results in more collisional excitations. Therefore, both the PRM and CM work more effectively than in the quiet atmosphere, leading to an overpopulation of the triplet levels corresponding to the He I 10 830 Å line.

However, if we introduce an electron beam, the optical depth of the chromosphere is drastically enhanced. Even in the quiet-Sun model, the electron beam can make the chromosphere very opaque. This is by virtue the result of nonthermal ionization of He I. We call this the collisional ionization-recombination mechanism, abbreviated as CRM. In order to show more clearly how the nonthermal electron beam influences the different transition processes to populate the triplet levels (levels 2 and 4) corresponding to the He I 10 830 Å line, we calculate the total transition rates from the PRM, CM and CRM, respectively, which are expressed as

$$T_{\rm PRM} = n_1 R_{1c} \frac{R_{c2} + R_{c4}}{\sum_{i=1}^{5} R_{ci}}, \tag{3}$$

$$T_{\rm CM} = n_1 (C_{12} + C_{14}), \tag{4}$$

and

$$T_{\rm CRM} = n_1 \left(C_{1c} + C_{1c}^{B}\right) \frac{R_{c2} + R_{c4}}{\sum_{i=1}^{5} R_{ci}}. \tag{5}$$

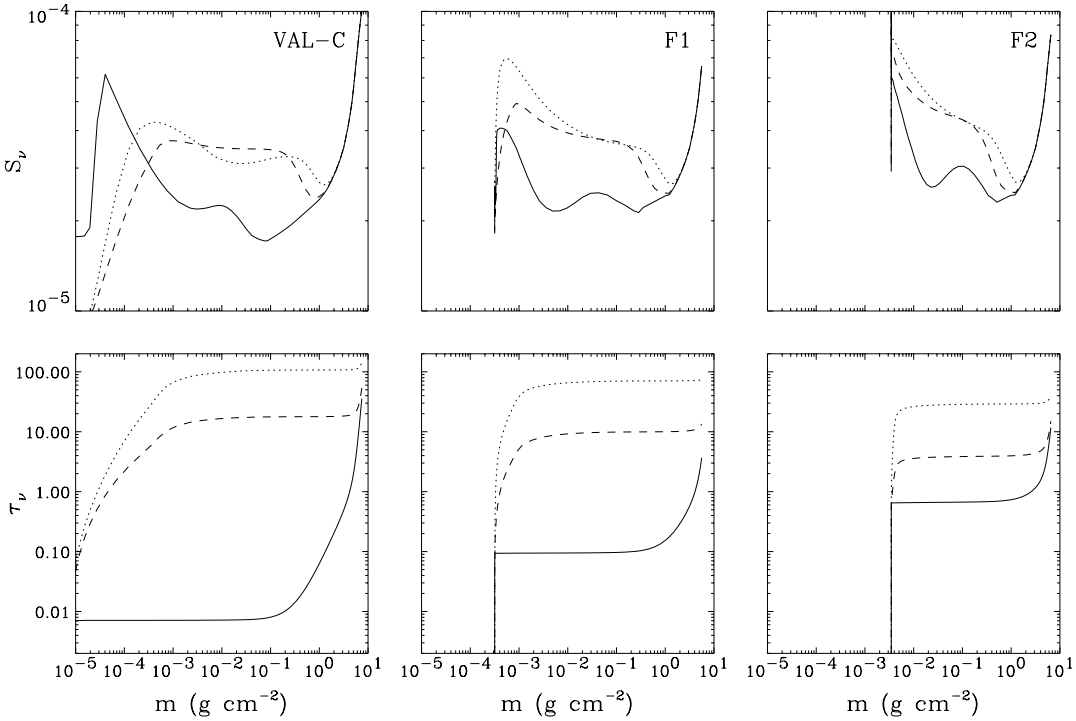

Fig. 3. Line source function and optical depth at 10 830.341 Å (the center of the strongest component of the He I 10 830 Å line) in different atmospheric models and for different cases of nonthermal electron beams. The quantities of S_ν are in units of erg cm^{-2} s^{-1} ster^{-1} Hz^{-1}. The line styles are the same as in Fig. 2.

In Fig. 4 we plot the results for two cases: without an electron beam and with a beam of energy flux 10^9 erg cm^{-2} s^{-1}. The figure shows that in the nonthermal case, the CRM is greatly enhanced and could even exceed the PRM and CM. The PRM can also be enhanced but is only a secondary effect following the enhanced EUV radiation resulting from the nonthermal ionization of He I.

On the other hand, the line source function also changes but in a slightly different manner. In the hot and condensed model (F2), the line source function mostly increases with height; but in the cool model (VAL-C), it may drop at the top of the chromosphere. Such a difference can be explained in terms of the two-level atom approximation, that is, the line source function is expressed as a linear combination of the mean radiative intensity and the local Planck function. In the VAL-C model, the mass density is relatively low and the line is almost radiation-dominated; thus the source function decreases towards upper layers of the chromosphere owing to efficient photon escaping. In the F2 model, the mass density is higher and the chromosphere becomes much more opaque, especially in the nonthermal case; therefore the source function keeps rising with height in the upper chromospheric layers. The change of the formation height and the source function for the He I 10 830 Å line in different models and in different thermal/nonthermal cases accounts for the computational results described above.

Note the specific shape of the line profile obtained for the F1 model in the case of a relatively strong electron beam with energy flux being 10^{10} erg cm^{-2} s^{-1}. The blue (10 829.081 Å) component and the red (10 830.250 and 10 830.341 Å) component both exhibit a central reversal; the central reversal in the red component is more pronounced, which makes the red component even less strong than the blue component. These features are of course caused by the opacity effects and the drop of the line source function at the top layers in the F1 atmosphere (see Fig. 3). Moreover, the profiles shown in Fig. 2 have not been convolved with a macro-turbulent velocity. If we convolve the computed profiles with a Gaussian macro-velocity of $\gtrsim$10 km s^{-1}, as was usually done, they will more likely match the observed ones.

3.2. Comparison with other models and observations

AJ97 investigated in detail the influence of the transition region structure, the coronal pressure (the column mass atop the atmosphere), and the coronal irradiation on the He I 10 830 Å line. In our computations, changing models from VAL-C to F1 and then to F2 reflects the effect of increasing the coronal pressure and the coronal irradiation. We find that the change of the profiles in the case without nonthermal effects, shown as solid lines in Fig. 2, is qualitatively consistent with the results revealed by AJ97.

There are currently not many spectroscopic observations of flares in the He I 10 830 Å line. Some previous observations have shown that the He I 10 830 Å line appears either in emission or in absorption in flare regions (e.g., Tandberg-Hanssen 1967; Harvey & Recely 1984; Li et al. 1996). In general, the former occurs preferentially in major flares while the latter in small flares. It has been reported, however, that the line can also go into emission in some small flares (Rust & Bridges 1975;

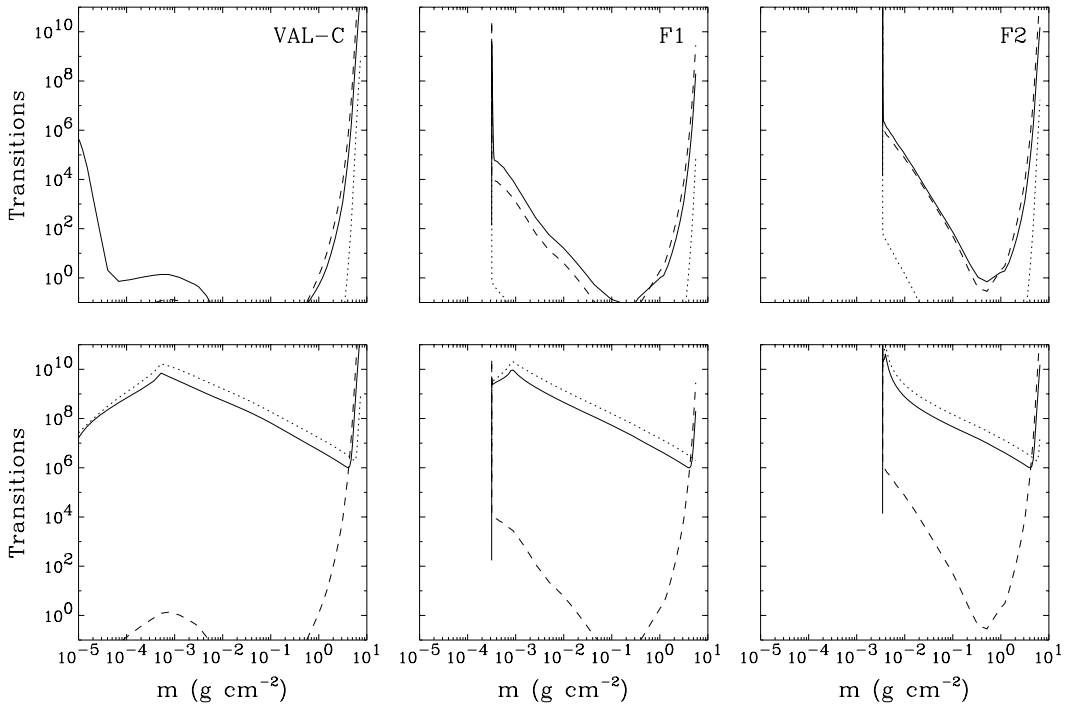

Fig. 4. Transitions to the triplet levels corresponding to the He I 10 830 Å line through three different processes: the photoionization-recombination mechanism (PRM, solid lines), the collisional mechanism (CM, dashed lines), and the collisional ionization-recombination mechanism (CRM, dotted lines). The upper panels show the case without an electron beam, while the lower panels are for the case with an electron beam of energy flux 10^9 erg cm^{-2} s^{-1}.

Penn & Kuhn 1995). These observational results are not surprising if considering the different nonthermal effects in each event. To check our computational results presented above, we need time-dependent spectroscopic observations for a flare.

3.3. Implications of the results

Observations have indicated that nonthermal electrons are usually accelerated during the impulsive phase of solar flares. The flaring atmosphere is heated by the impact of nonthermal electrons and/or by heat conduction. Our computational results imply that whether the He I 10 830 Å line is in absorption or in emission depends on the heating status of the flaring atmosphere and the strength of the electron beam. Therefore, we propose the following scenario for the evolution of the He I 10 830 Å line during a solar flare. At first, when the flare originally occurs, nonthermal electrons begin to be accelerated and to bombard the lower atmosphere which has not been heated substantially; the He I 10 830 Å line changes from weak absorption to strong absorption. With the flare development, the chromosphere becomes gradually heated and condensed, the line then turns from absorption to emission; the emission increases if the electron beam keeps working. We note that, if there is no nonthermal effect, the line profiles from the three model atmospheres also show a similar variation behavior with, however, much less amplitude of absorption and emission in the above two cases. Therefore, we think that a strong absorption at the early phase and a strong emission at the maximum phase can be regarded as evidence of nonthermal effects. The He I 10 830 Å line can be used as a diagnostic tool for nonthermal effects if combined with other lines and hard X-ray observations.

4. Conclusions

The purpose of this paper is to investigate the formation and properties of the He I 10 830 Å line in a flaring atmosphere. We obtain the line profiles with non-LTE calculations for different model atmospheres with and without nonthermal effects by an electron beam. As expected, if the nonthermal effects are not included, the line is very weak in absorption in a cool atmosphere while it turns to emission in a hot and condensed atmosphere. However, the presence of an electron beam can significantly change the line strength, producing much stronger absorption and emission in these two cases. By analyzing in detail the transition processes between the atomic levels of He I, we find that in the nonthermal case the collisional ionizations of He I are greatly enhanced. Therefore, in addition to the other two processes previously known (i.e., the photoionization-recombination and the collisional excitation), the collisional ionization followed by recombinations can act as an important agent in populating the triplet levels corresponding to the He I 10 830 Å line. With nonthermal effects, the chromosphere usually becomes optically thick in this line. These results suggest that the He I 10 830 Å line is rather sensitive to nonthermal effects. In particular, we suggest that a strong absorption at an early time and a strong emission at the maximum time during a flare could be regarded as a signature of nonthermal effects. This line is therefore a potential diagnostic tool for nonthermal effects in solar and stellar flares. Since

the nonthermal effects usually work together with some other effects like an enhanced EUV irradiation and a high coronal pressure (AJ97), multi-line spectroscopy is required for discrimination between them.

Acknowledgements. We are grateful to the referee for valuable comments that helped improve the paper. This work was supported by NKBRSF under grant G20000784, by NSFC under grants 10025315, 10221001, and 10333040, and by a grant from TRAPOYT.

References

Andretta, V., & Jones, H. P. 1997, ApJ, 489, 375
Avrett, E. H., Fontenla, J. M., & Loeser, R. 1994, IAU Symp., 154, 35
Benson, R. S., & Kulander, J. L. 1972, Sol. Phys., 27, 305
Dimitrijević, M. S., & Sahal-Bréchot, S. 1984, JQSRT, 31, 301
Ding, M. D., & Fang, C. 2000, MNRAS, 317, 867
Ding, M. D., & Schleicher, H. 1997, A&A, 322, 674
Ding, M. D., Qiu, J., & Wang, H. 2002, ApJ, 576, L83
Ding, M. D., Liu, Y., Yeh, C.-T., & Li, J. P. 2003, A&A, 403, 1151
Fang, C., Hénoux, J. C., & Gan, W. Q. 1993, A&A, 274, 917
Fernley, J. A., Taylor, K. T., & Seaton, M. J. 1987, J. Phys. B, 20, 6457
Fontenla, J. M., Avrett, E. H., & Loeser, R. 1993, ApJ, 406, 319
Griem, H. R. 1974, Spectral Line Broadening by Plasmas (New York: Acad. Press)
Harvey, K. L., & Recely, F. 1984, Sol. Phys., 91, 127
Hénoux, J. C., Fang, C., & Gan, W. Q. 1995, A&A, 297, 574
Kono, A., & Hattori, S. 1984, Phys. Rev. A, 29, 2981
Labrosse, N., & Gouttebroze, P. 2001, A&A, 380, 323
Li, H., Fan, Z., & You, J. 1996, Chinese Astron. Astrophys., 20, 85
Machado, M. E., Avrett, E. H., Vernazza, J. E., & Noyes, R. W. 1980, ApJ, 242, 336
Martin, W. C. 1987, Phys. Rev. A, 36, 3575
Mihalas, D. 1978, Stellar Atmospheres (San Francisco: W. H. Freeman and Company)
Mihalas, D., & Stone, M. E. 1968, ApJ, 151, 293
Milkey, R. W., Heasley, J. N., & Beebe, H. A. 1973, ApJ, 186, 1043
Penn, M. J., & Kuhn, J. R. 1995, ApJ, 441, L51
Rust, D. M., & Bridges, C. A. 1975, Sol. Phys., 43, 129
Sasselov, D. D., & Lester, J. B. 1994, ApJ, 423, 785
Shine, R., Gerola, H., & Linsky, J. L. 1975, ApJ, 202, L101
Tandberg-Hanssen, E. 1967, Solar Activity (Waltham, MA: Blaisdell)
Vernazza, J. E., Avrett, E. H., & Loeser, R. 1981, ApJS, 45, 635
You, J., Wang, C., Fan, Z., & Li, H. 1998, Sol. Phys., 182, 431